

OncoReason: Structuring Clinical Reasoning in LLMs for Robust and Interpretable Survival Prediction

Raghu Vamshi Hemadri,
Geetha Krishna Guruju, Kristi Topollai, Anna Ewa Choromanska

New York University, Tandon School of Engineering
 {rh3884, gg3039, kt2664, ac5455}@nyu.edu

Abstract

Predicting cancer treatment outcomes requires models that are both accurate and interpretable, particularly in the presence of heterogeneous clinical data. While large language models (LLMs) have shown strong performance in biomedical NLP, they often lack structured reasoning capabilities critical for high-stakes decision support. We present a unified, multi-task learning framework that aligns autoregressive LLMs with clinical reasoning for outcome prediction on the MSK-CHORD dataset. Our models are trained to jointly perform binary survival classification, continuous survival time regression, and natural language rationale generation. We evaluate three alignment strategies: (1) standard supervised fine-tuning (SFT), (2) SFT with Chain-of-Thought (CoT) prompting to elicit step-by-step reasoning, and (3) Group Relative Policy Optimization (GRPO), a reinforcement learning method that aligns model outputs to expert-derived reasoning trajectories. Experiments with LLaMa3-8B and Med42-8B backbones demonstrate that CoT prompting improves F1 by +6.0 and reduces MAE by 12%, while GRPO achieves state-of-the-art interpretability and predictive performance across BLEU, ROUGE, and BERTScore. We further show that existing biomedical LLMs often fail to produce valid reasoning traces due to architectural constraints. Our findings underscore the importance of reasoning-aware alignment in multi-task clinical modeling and set a new benchmark for interpretable, trustworthy LLMs in precision oncology.

Introduction

Cancer remains one of the most complex and heterogeneous diseases, with treatment outcomes varying dramatically across patients, even within the same diagnostic category (Hanahan and Weinberg 2011; Marusyk, Almendro, and Polyak 2012). Clinical decisions, such as therapy selection, outcome prediction, and risk assessment, rely on physician experience, clinical guidelines, and population models (Topol 2019). However, these approaches often fall short in personalizing treatment or explaining predictions, especially in rare or high-risk cases (Esteva et al. 2019; Yala et al. 2021).

While EHRs, radiology, and pathology data contain valuable context, much of this information remains underused due to its unstructured nature (Jensen, Jensen, and Brunak 2012; Alsentzer et al. 2019). Traditional models like Cox regression and GBDTs handle structured features well but fail

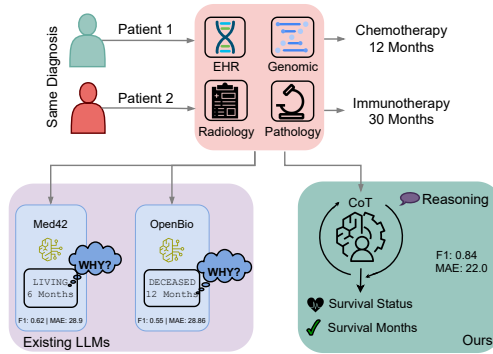


Figure 1: **From Black-Box Models to Reasoning-Augmented LLMs for Cancer Outcome Prediction.** Existing LLMs excel at general biomedical tasks but lack structured clinical reasoning and explainability. Our proposed framework augments LLMs with Chain-of-Thought (CoT) prompting and GRPO-based alignment to perform interpretable, multi-task survival prediction on MSK-CHORD.

to incorporate long-range dependencies and semantic richness from clinical narratives (Rajkomar et al. 2018; Boag et al. 2018). Moreover, their opaque predictions hinder interpretability, which is crucial for real-world oncology (Caruana et al. 2015; Tonekaboni et al. 2019).

LLMs pretrained on biomedical corpora offer a pathway to integrate structured and unstructured data into a unified representation. Models such as Med42-8B (Christophe et al. 2024), MEDITRON (Chen et al. 2023), and OPENBIO (Ankit Pal 2024) have shown promise in biomedical tasks like QA and summarization, yet are not optimized for structured clinical inference and explainability.

Figure 1 illustrates a key limitation of existing LLMs in oncology: while they can predict survival status or duration (e.g., “Living: 6 months”), they often fail to provide clinical justifications, reducing interpretability. To address this gap, we propose **OncoReason**, a reasoning-aligned LLM framework designed to generate patient-specific rationales alongside outcome predictions, enhancing transparency in high-stakes cancer care. We fine-tune open-source LLM backbones (LLaMa3-8B, Med42-8B) on the MSK-CHORD

dataset (Jee et al. 2024) using a unified, auto-regressive multi-task protocol that jointly predicts (1) binary survival status, (2) continuous survival months, and (3) natural language Chain-of-Thought (CoT) rationales.

To assess the impact of reasoning-aware learning, we compare three training strategies: (1) Supervised Fine-Tuning (SFT) without CoT, (2) SFT with CoT prompting (Wei et al. 2022), and (3) Group Relative Policy Optimization (GRPO), a reinforcement-based alignment method that uses diverse CoT exemplars to encourage causal and calibrated inference (Shao et al. 2024). We show that reasoning-augmented models significantly outperform strong biomedical LLM baselines across classification, regression, and generation metrics, while also improving the semantic fidelity and reliability of model explanations (Huang et al. 2023). Our contributions are summarized as follows:

- We propose a unified training pipeline for jointly modeling survival status, survival duration, and Chain-of-Thought reasoning in cancer outcome prediction.
- We conduct extensive evaluations on the MSK-CHORD dataset, showing that our reasoning-enhanced models outperform leading clinical LLMs on all fronts, including precision, MAE/RMSE, BLEU, ROUGE, and BERTScore.

Our work paves the way for next-generation clinical AI systems that not only predict outcomes but also communicate the rationale behind each decision, making them more trustworthy and robust in real-world oncology workflows.

Related Work

Treatment outcome prediction involves forecasting the results of medical interventions, aiming to anticipate a patient’s response to a specific treatment regimen. In oncology, this task is especially significant due to the heterogeneity of cancer types and patient responses. Predictive models help identify which patients may benefit from therapies such as chemotherapy, immunotherapy, or targeted treatments, enabling personalized care.

Treatment outcome prediction has traditionally relied on statistical and machine learning models. Traditional statistical approaches like Cox regression (Cox 1992) and logistic regression (Hos 2000) are valued for simplicity and interpretability but often make strong assumptions (e.g., linearity or proportional hazards) and may underperform in high-dimensional settings. Tree-based models like Random Forests and XGBoost (Breiman 2001; Friedman 2001) capture nonlinear patterns and improve performance, but at the cost of interpretability.

Recent advances in deep learning have transformed outcome prediction by enabling models to capture complex, high-dimensional patterns. CNNs have proven effective in medical imaging by extracting hierarchical features, though their reliance on annotated data and opaque predictions limits clinical trust (Litjens et al. 2017). Hybrid approaches have integrated structured variables with imaging data (Sonntag and Profitlich 2019). Models like Deep Patient (Zhang et al. 2016) and Doctor AI (Kazachkov 2015) have leveraged

unsupervised and sequential learning from EHRs to forecast patient trajectories.

The emergence of large language models (LLMs) has also significantly advanced NLP in medicine. GPT-4 has enabled complex tasks such as diagnostic reasoning and risk assessment (OpenAI and et. al. 2024), while Med-PaLM has reached near-human performance in medical QA (Zitu et al. 2024). Biomedical-adapted models such as BioBERT and ClinicalBERT (Nazi and Peng 2024) have improved diagnosis and summarization through pretraining on clinical corpora. More recently, LLMs have been applied to treatment outcome prediction using both structured and unstructured inputs. Prompting-based methods enable zero-shot forecasting of outcomes like mortality and readmission (Zhu et al. 2024), and domain-adapted models like MEDITRON, OPENBIO, and Med42-8B have become strong clinical baselines.

Several studies have explored LLMs in oncology and prognosis: (PMC 2023) focused on biomarker analysis; (Chen and Brown 2023) compared transformers with traditional models; and (Naik, Feldman, and Hope 2021; Zheng, Xu, and Fu 2024; Shoham 2023; Zakka and Chaurasia 2023) proposed multimodal and guideline-integrated frameworks for forecasting and recommendations. These works highlight the need for methods that unify reasoning, robustness, and interpretability, core to our approach.

LLMs also raise concerns around interpretability, as black-box predictions can hinder clinical adoption (Lyu et al. 2024). Bias in training data may reinforce inequities (Ong et al. 2024), and regulatory challenges require strong privacy protections. In response, recent efforts have targeted transparency: (Arasteh and Lotfinia 2023) assessed ChatGPT ADA for ML workflows; (Xue and Abraham 2024) fine-tuned BioGPT and ClinicalBERT for postoperative risk; and (Gu 2024b,a) advanced prompt engineering and developed NYUTron for EHR forecasting. Other works have focused on interpretable model design (Tian and Patel 2023), personalized treatment (Wang and Zhao 2024), and bias mitigation using diverse datasets (Singh and Brown 2024).

Further research explores integrating multimodal data to boost prediction. (Zhou et al. 2021) combined clinical, genomic, and imaging data for immunotherapy modeling, while (Torkamani et al. 2020; Jiang et al. 2022) stressed the value of genetic features in precision oncology. Ensemble and neural network models have been used to model gene-treatment interactions (Chen et al. 2020), and (Kim et al. 2023) used EHR data for predicting outcomes in chronic diseases with oncology applications. Although LLMs offer a promising path forward, challenges like missing data, fine-tuning complexity, and domain generalizability persist. Future research must prioritize robust training pipelines, comprehensive multimodal datasets, and rigorous validation, directions explored in recent forecasting and LLM studies (Kraljevic et al. 2024; Clusmann et al. 2023).

Dataset Description

We utilize the **MSK-CHORD** dataset (Jee and et. al 2024; Fong et al. 2024b), a publicly available oncology dataset curated by Memorial Sloan Kettering Cancer Center (MSKCC) via cBioPortal that provides a rich repository

of patient demographics, disease progression, treatment history, molecular profiling, and survival outcomes, making it highly suitable for predictive modeling in clinical oncology.

Data Overview and Preparation

We begin with the full patient cohort and use an 80:20 split for training and evaluation. Each record, in JSON format, includes key clinical attributes such as demographics, cancer staging, treatment regimens (e.g., chemotherapy, immunotherapy), and survival outcomes. Laboratory markers (e.g., CEA, CA15-3) and biomarker profiles (e.g., PD-L1, HER2) are also included where available. Further details on the feature schema are provided in the Appendix. For use with LLMs, we convert each structured record into a natural language prompt comprising a task description, a cancer-type-specific patient summary from dynamically selected attributes, and the prediction targets: survival status (binary) and estimated survival duration (in months).

Attribute Selection and Summary Construction

To reduce input length while retaining relevance, we dynamically select clinical features based on cancer type. For example, summaries for breast cancer prioritize hormone receptor status and tumor markers (e.g., HER2, CA15-3), while NSCLC records emphasize smoking history and PD-L1 expression. These selections are guided by attribute metadata and cancer-specific heuristics.

Furthermore, we generate concise, cancer-type-specific natural-language summaries by extracting and formatting key clinical attributes (e.g., stage, age, sex, smoking history), relevant biomarkers (e.g., HER2, PD-L1), tumor site indicators, treatment histories (chemotherapy, immunotherapy), sample-specific histological and diagnostic details, and longitudinal tumor marker trends (e.g., CEA, CA19-9 via simple regression). Irrelevant fields are filtered using metadata flags and disease-specific heuristics. These structured summaries, paired with survival outcomes, are then passed to an LLM to produce clinically interpretable reasoning traces.

Chain-of-Thought Reasoning Trace Generation

We leverage large-scale models such as DeepSeek R1 (Mondillo et al. 2025; DeepSeek-AI and et. al. 2025) to generate chain-of-thought (CoT) reasoning traces (Lu et al. 2022; Hu et al. 2024; Li et al. 2024) for all samples. These traces decompose each prediction into clinically interpretable steps, assessing cancer stage and diagnosis to establish baseline prognosis and likely disease trajectory; evaluating patient-specific factors (e.g., age, sex, treatment eligibility); reviewing temporal biomarker patterns and tumor marker trends to infer progression or response; analyzing systemic and local treatment regimens (chemotherapy, immunotherapy, radiation, investigational agents) to gauge therapeutic intensity; and synthesizing evidence holistically to estimate survival outcomes, while maintaining computational efficiency for large-scale processing. Each CoT output is accompanied by a commentary on clinical uncertainties, highlighting missing or incomplete data, ambiguous staging, or unclear treatment timelines, to enhance transparency and alignment with domain expertise (Fong et al. 2024a).

Chain-of-Thought Evaluation via Embedding-Based Metrics

To assess the quality of CoT explanations generated across 24,950 patient records, we conducted an automatic evaluation using sentence-transformer-based semantic similarity. Each CoT trace was assessed for: (i) step-to-summary relevance, (ii) intra-step coherence, and (iii) prompt repetition, using cosine similarity scores computed from BERT-based sentence embeddings (Reimers and Gurevych 2019).

Table 1: Evaluation of Chain-of-Thought (CoT) reasoning traces across 24,950 cancer patient summaries using BERT-based similarity metrics.

Metric	Mean	Std Dev	Min	Max
AVERAGE RELEVANCE	0.537	0.048	0.332	0.745
MINIMUM RELEVANCE	0.394	0.081	0.008	0.721
AVERAGE COHERENCE	0.463	0.067	0.179	0.812
MAX PROMPT OVERLAP	0.306	0.041	0.160	0.460
NUMBER OF STEPS	6.10	0.92	3.00	14.00

Overall, as shown in Table 6, CoT traces achieved an average relevance of 0.537, coherence of 0.463, and prompt overlap of 0.306, indicating well-grounded, logically continuous, and context-specific reasoning. Stratifying by cancer type (Table 7) reveals meaningful variation: pancreatic traces were most relevant (0.567), prostate traces most coherent (0.491), lung cancer used the fewest reasoning steps (5.88), and colorectal the most verbose (6.33), with prompt overlap staying below 0.34 across all five types. These findings confirm that our CoT strategy preserves fidelity and adaptability across diverse oncology settings.

Table 2: Mean BERT-based metrics for CoT quality across cancer types.

Cancer Type	Avg Relevance	Avg Coherence	Prompt Overlap
BREAST	0.525	0.447	0.308
COLORECTAL	0.525	0.458	0.305
NSCLC (LUNG)	0.538	0.465	0.295
PANCREATIC	0.567	0.465	0.301
PROSTATE	0.547	0.491	0.333

Method

In this work, we explore three distinct approaches for treatment outcome prediction and survival time estimation using the MSK-CHORD dataset. Our objective is not only to predict the binary outcome, 0 for *LIVING* and 1 for *DECEASED*, but also to estimate the number of survival months post treatment, while simultaneously incorporating interpretable reasoning into the prediction process (Langbein et al. 2024). Importantly, all fine-tuning is performed in an *autoregressive* manner (Radford et al. 2019), where the model is trained to generate outputs token-by-token conditioned on prior tokens.

Autoregressive Fine-Tuning for Treatment Outcome Prediction

In this approach, we fine-tune the LLaMa 3 model (Hou et al. 2024; et. al. 2024) on the MSK-CHORD dataset to perform direct cancer clinical outcome prediction without generating an intermediate chain-of-thought. The task is formulated as a sequence-to-sequence prediction problem where the model is conditioned on a structured prompt describing the patient’s clinical data. The prompt emphasizes key factors such as disease stage, tumor sites, patient age, smoking history, cancer type, and treatment details, and instructs the model to output a concise prediction comprising:

- **Overall Survival Status:** A binary label where 0: LIVING indicates survival and 1: DECEASED indicates death.
- **Estimated Overall Survival:** A float value representing the estimated survival time in months.

To align the model’s output with clinical requirements, we adopt a prompt that explicitly delineates the expected response format. An example of the prompt used during training is provided in Appendix. By leveraging autoregressive fine-tuning on carefully curated prompts, our method achieves a robust mapping from heterogeneous clinical data to outcome predictions (Henriksson et al. 2023), forming a foundational baseline upon which more sophisticated reasoning models (incorporating chain-of-thought and reinforcement learning) may be compared (Gema et al. 2024).

Supervised Fine-Tuning with Chain-of-Thought Distillation

Our second approach augments the standard supervised fine-tuning (SFT) framework by incorporating an interpretable chain-of-thought (CoT) mechanism distilled from a high-capacity reasoning model (e.g., DeepSeek-R1). In this setting, a teacher model generates intermediate reasoning steps, denoted as z^* , for each input x drawn from the MSK-CHORD dataset. These intermediate tokens are leveraged to guide the student model in both learning to predict treatment outcomes, with binary labels (0: LIVING or 1: DECEASED) and a regression task estimating survival months, and in producing explicit, human-interpretable reasoning trajectories (Phan et al. 2023).

Formally, given an input x , the student model generates a chain-of-thought $z = g_\theta^{\text{CoT}}(x)$ alongside its clinical prediction y . To align the student’s reasoning with the teacher-provided trace, we incorporate an auxiliary loss defined as:

$$\mathcal{L}_{\text{CoT}}(z, z^*) = D(z, z^*),$$

where $D(\cdot, \cdot)$ represents a divergence metric (e.g., token-level cross-entropy or KL-divergence). The overall objective function is then formulated as:

$$\mathcal{L}_{\text{SFT+CoT}}(\theta) = \mathcal{L}_{\text{SFT}}(\theta) + \lambda_{\text{CoT}} \mathcal{L}_{\text{CoT}}(z, z^*),$$

with λ_{CoT} serving as a hyperparameter that balances the fidelity of the predictive output with the alignment of the reasoning process.

This autoregressive loss is optimized via teacher forcing, ensuring that at each decoding step the model is conditioned

on the ground-truth token sequence. This training strategy facilitates the learning of a coherent and logically structured chain-of-thought that not only underpins the final clinical prediction but also provides an explicit rationale that can be audited, a crucial requirement in medical decision support systems (Yang et al. 2024; He, Tang, and Wang 2024).

Embedding intermediate reasoning within the model’s output enhances interpretability by exposing the clinical rationale behind predictions. The multi-task setup, jointly modeling classification and regression, helps the model capture dependencies between reasoning and outcomes. Additionally, distilling chains of thought from a larger teacher model boosts accuracy and generalization. Drawing from advances in reasoning alignment, and using the expressivity of LLaMA3 and diversity of MSK CHORD, our approach offers robust and interpretable survival prediction, paving the way for further refinement through distillation and reinforcement learning.

Cold-Start SFT with GRPO for Joint Reasoning and Prediction

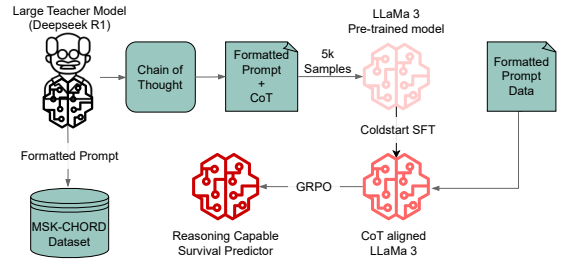


Figure 2: This diagram illustrates the methodology applied to train survival predictor on the MSK-CHORD dataset, using GRPO.

Our third approach as shown in Fig. 2, introduces a two-stage framework that leverages teacher-generated Chain-of-Thought (CoT) annotations and reinforcement learning to enhance both prediction accuracy and the interpretability of reasoning. The method is specifically designed to predict treatment outcomes (0: LIVING, 1: DECEASED) and to estimate post-treatment survival months using the dataset.

Cold-Start Supervised Fine-Tuning with CoT In the first stage, we perform supervised fine-tuning (SFT) on approximately 80% of the MSK-CHORD dataset. Each sample is paired with a teacher-generated CoT annotation that encapsulates the reasoning behind the prediction. This cold-start phase is intended to:

- **Impart Structured Reasoning:** By learning from high-quality, expert-curated CoT annotations, the model acquires an initial capability to reason about treatment outcomes.
- **Facilitate Subsequent Optimization:** The preliminary training creates a favorable starting point for further refinement via RL, mitigating the instability typically associated with cold-start RL from scratch.

Generalized Reward Policy Optimization (GRPO) To refine reasoning and outcome alignment, we employ Generalized Reward Policy Optimization (GRPO) (Shao et al. 2024), a reinforcement learning method that eliminates the need for a value critic by leveraging group-based relative rewards. Its efficient, variance-reduced training objective facilitates stable policy optimization in our outcome reasoning task. Formulation details are provided in the Appendix .

Reinforcement Learning via Generalized Reward Policy Optimization (GRPO) Following the cold-start SFT, the model is further optimized using Generalized Reward Policy Optimization (GRPO), as described in Subsection-*GRPO*. In this phase, we jointly refine both the reasoning process and the final predictions by incorporating a reward signal that reinforces consistency and coherence.

Let z denote the generated chain-of-thought for input x , where $f_\theta(x)$ is the predicted binary outcome (0 for *LIVING*, 1 for *DECEASED*) and $g_\theta(x)$ is the predicted survival time in months. The GRPO objective is:

$$\mathcal{L}_{\text{GRPO}}(\theta) = \mathcal{L}_{\text{SFT+CoT}}(\theta) - \beta \cdot R(z, f_\theta(x), g_\theta(x)), \quad (1)$$

where β is a scaling hyperparameter and $R(\cdot)$ is the total reward for a given sample.

This formulation encourages the model to generate accurate predictions supported by coherent, structured rationales.

Multi-Faceted Reward Function To guide GRPO optimization, we define a composite reward function $R(\cdot)$ that evaluates each generated output along four axes:

- **Correctness Reward** (R_{correct}): Assigned 1.0 if both the predicted binary outcome $f_\theta(x)$ and estimated survival time $g_\theta(x)$ exactly match the ground truth; 0.0 otherwise.
- **Integer Validity Reward** (R_{int}): This reward checks whether the extracted survival time is a valid integer. A partial reward (0.5) is provided for a well-formed integer.
- **Strict Format Reward** (R_{strict}): Assigned 0.5 if the output strictly adheres to the following XML-like schema:

```

<reasoning>
  ...
  (chain-of-thought text) ...
</reasoning>
<answer>
  ...
  (final prediction) ...
</answer>

```

- **Soft Format Reward** (R_{soft}): Grants 0.5 if the output conforms to a relaxed variant of the required structure, allowing minor structural deviations while still promoting a coherent output style.

The total reward is computed as:

$$R = R_{\text{correct}} + R_{\text{int}} + R_{\text{strict}} + R_{\text{soft}}.$$

The correctness and integer rewards directly impact predictive accuracy, while the format rewards ensure the chain-of-thought remains interpretable and structured. By integrating these signals, GRPO effectively promotes the emergence of coherent reasoning alongside accurate treatment outcome predictions and survival time estimates.

In summary, the approach in Subsection-*RL via GRPO* combines the strengths of supervised fine-tuning with teacher-generated CoT annotations and the flexibility of reinforcement learning via GRPO. This method not only refines predictive performance on the MSK-CHORD dataset but also endows the model with a transparent and robust reasoning process, paving the way for more interpretable and clinically actionable treatment outcome predictions.

Experiments

Training

We adopt a unified, auto-regressive multi-model training protocol on the MSK-CHORD dataset. Specifically, we train three distinct variants: (1) Supervised Fine-Tuning (SFT) without chain-of-thought (CoT), (2) SFT with CoT prompting, and (3) Group Relative Policy Optimization (GRPO) with CoT cold-start initialization. Each variant is initialized from one of two backbone models: LLaMa3-8B or Med42-8B, allowing for a comparative evaluation across model foundations. Full hardware and experimental settings are provided in Appendix . As well as sample model inputs and outputs for all methods described.

SFT Training First, we perform SFT with and without CoT prompting. Each instance is initialized from either LLaMa3-8B or Med42-8B and trained to jointly perform classification and regression in an auto-regressive manner. The model predicts: a binary value for survival status (0 = living, 1 = deceased) and a regressed value for estimated survival months. A multi-task loss is used, as defined in Subsection-*SFT with Chain-of-Thought Distillation*.

GRPO Training To incorporate structured reasoning, we generate CoT trajectories on 20K held-out samples using DeepSeek-R1 (Lu et al. 2024). From these trajectories, we extract the penultimate hidden states of LLaMa3-8B $h_i \in \mathbb{R}^d$ and perform K-Means clustering with $K = 5000$ to identify diverse “cold-start” exemplars $\{\mu_j\}_{j=1}^{5000}$ (MacQueen 1967) that summarize the spectrum of reasoning patterns. These closest examples to each of these 5000 cluster centers form the initial batch for GRPO, ensuring the policy sees a representative subset before fine-tuning on the full dataset (Liu et al. 2023). We treat the SFT model as a policy that emits both reasoning traces and final predictions, and optimize it using the GRPO loss described in Subsection-*Reinforcement Learning via GRPO*.

Survival Status Prediction

To assess binary survival status classification, we report standard metrics (Precision, Recall, F1) with and without Chain-of-Thought (CoT) prompting across baselines (MEDITRON, OPENBIO, MED42) and our fine-tuned models (OURS (LLAMA3), OURS (MED42)), with and without GRPO reinforcement optimization (Table 3). CoT consistently improves performance: MED42 gains marginally (F1: 0.62→0.63), while our models show notable boosts—OURS (MED42) from 0.77 to 0.81 and OURS (LLAMA3) from 0.77 to 0.83. GRPO further enhances results, with OURS

Table 3: Classification metrics (Precision, Recall, F1-score) for survival status prediction. Metrics are grouped by Chain-of-Thought (CoT) prompting.

Model	Without CoT			With CoT		
	Precision	Recall	F1	Precision	Recall	F1
MEDITRON	0.53	0.53	0.50	0.57	0.52	0.42
OPENBIO	0.74	0.61	0.55	0.75	0.61	0.52
MED42	0.63	0.63	0.62	0.71	0.66	0.63
DEEPEEK R1	0.62	0.75	0.68	—	—	—
OURS (MED42)	0.77	0.77	0.77	0.81	0.80	0.81
<i>Ours (Med42) (GRPO)</i>	—	—	—	0.82	0.80	0.81
OURS (LLAMA3)	0.77	0.77	0.77	0.84	0.82	0.83
<i>Ours (LLaMa3) (GRPO)</i>	—	—	—	0.84	0.83	0.84

(LLAMA3) (GRPO) achieving the highest F1 (0.84), precision (0.84), and recall (0.83). Supporting ROC curves are in Appendix .

Survival Months Prediction

Table 4: Regression metrics (MAE, RMSE) for survival months prediction. Smaller values are better. Metrics are grouped by CoT (Chain-of-Thought) prompting.

Model	Without CoT		With CoT	
	MAE ↓	RMSE ↓	MAE ↓	RMSE ↓
MEDITRON	30.36	40.74	35.38	47.01
OPENBIO	28.86	39.67	30.05	40.46
MED42	28.90	39.08	29.27	40.78
DEEPEEK R1	26.76	37.87	—	—
OURS (MED42)	22.91	33.19	23.69	33.54
<i>—GRPO</i>	—	—	22.30	32.80
OURS (LLAMA3)	24.05	34.72	24.01	34.13
<i>—GRPO</i>	—	—	22.00	32.40

To assess survival time estimation, we report MAE and RMSE across model variants in Table 4. Baseline models like MED42, MEDITRON, and OPENBIO show higher error (MAE 28.86–35.38), with CoT prompting offering only minor improvements. In contrast, our fine-tuned models substantially reduce both MAE and RMSE. With CoT, OURS (LLAMA3) achieves 24.01 (MAE) and 34.13 (RMSE), while OURS (MED42) reaches 23.69 and 33.54. GRPO further boosts performance: OURS (MED42)(GRPO) and OURS (LLAMA3)(GRPO) attain the best results, with the latter achieving 22.00 (MAE) and 32.40 (RMSE).

Figure 3 shows reduced median and variance in absolute errors for CoT-enhanced models, with GRPO variants exhibiting the tightest spreads. In Figure 4, our LLaMa3-based model aligns closely with the identity line, showing improved calibration over baselines like MED42, which underestimates high-survival cases. These results confirm that CoT prompting and GRPO alignment significantly improve outcome prediction in terms of accuracy and robustness.

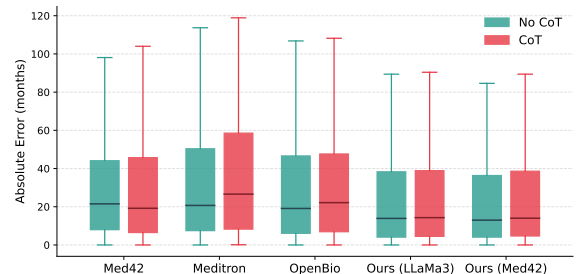


Figure 3: Absolute error distribution (in months) for all models with and without CoT prompting. CoT-enhanced models show reduced median and variance.

Chain of Thought for Interpretability

To assess the interpretability and reasoning capability of our models, we evaluate CoT generations using BLEU (Papineni et al. 2002), ROUGE (Lin 2004), and BERTScore F1 (Zhang et al. 2020). These metrics quantify both lexical overlap and semantic alignment between the model-generated rationales and ground truth annotations.

Table 5: Text generation results under Chain-of-Thought (CoT) prompting. All models in this table used CoT.

Model	BLEU	ROUGE-L	BERT-F1
MEDITRON	10.28	0.082	-0.306
OPENBIO	13.08	0.172	0.120
MED42	57.95	0.241	0.240
DEEPEEK R1	31.44	0.166	0.038
OURS (MED42)	95.88	0.363	0.438
<i>—GRPO</i>	98.00	0.368	0.442
OURS (LLAMA3)	97.41	0.364	0.438
<i>—GRPO</i>	98.15	0.370	0.443

As shown in Table 5, our models, especially those trained with GRPO, achieve state-of-the-art results across all metrics. OURS (LLAMA3)(GRPO) achieves BLEU 98.15 and BERT-F1 0.443, far surpassing strong baselines like MED42 (BLEU 57.95, BERT-F1 0.240), and outperforming underperformers such as MEDITRON and OPENBIO, whose BLEU scores fall below 15. Robustness is demonstrated by

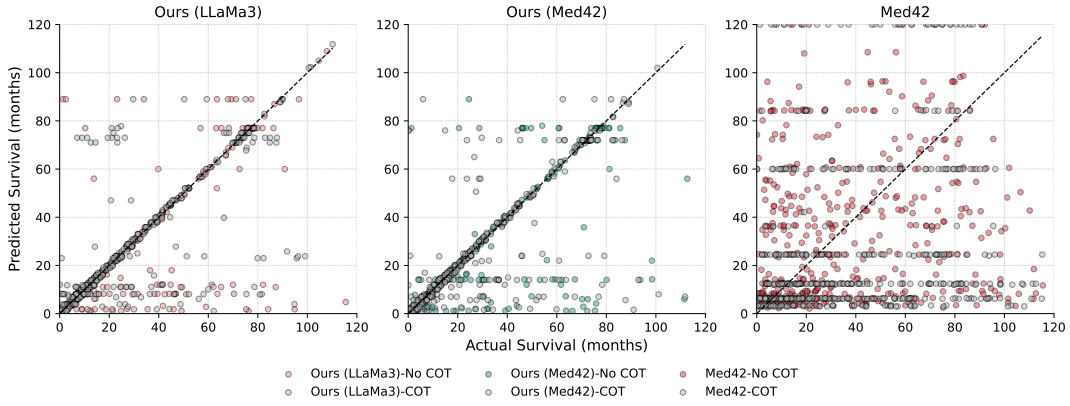


Figure 4: Predicted vs. actual survival months for OURS (LLAMA3), OURS (MED42), and MED42 baselines. The dashed line indicates perfect prediction.

100% CoT response rates for all our variants, with or without GRPO, in contrast to substantial failure rates in MEDITRON (1911) and OPENBIO (1854). (see Appendix)

Figures 5 and 6 highlight quality differences and show a clear positive correlation between BLEU and Macro-F1, linking interpretability to predictive accuracy. CoT generation failures in baseline LLMs stem from architectural constraints such as limited context length and poor support for structured reasoning. Attempts using ReACT (Yao et al. 2022) scaffolding were insufficient to overcome these issues. In contrast, GRPO-aligned models generate complete and valid CoT traces for all inputs.

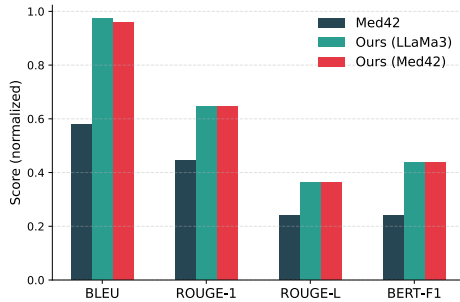


Figure 5: Generation quality under CoT prompting, evaluated via BLEU, ROUGE, and BERTScore.

These findings affirm that successful CoT prompting for clinical interpretability not only depends on prompt engineering but also on architectural adaptability and optimization strategies. GRPO ensures coherent reasoning, semantic fidelity, and reliable end-to-end performance for interpretable medical AI.

Conclusion

In this work, we present a unified framework for cancer treatment outcome prediction using LLMs, addressing key limitations of current clinical AI. Leveraging the MSK-CHORD dataset, our method combines SFT and GRPO,

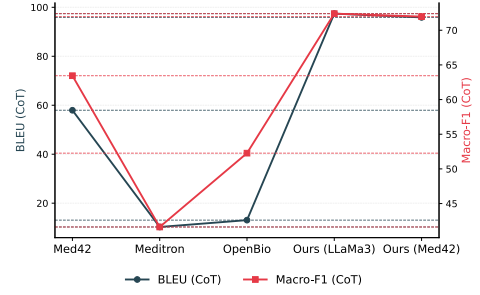


Figure 6: Correlation between reasoning quality (BLEU) and classification accuracy (Macro-F1) under CoT prompts.

with and without Chain-of-Thought (CoT) prompting. By integrating chain-of-thought rationales with accurate survival predictions, OncoReason enhances transparency and trust in oncology AI-enabling clinicians to audit and deploy outputs confidently in high-stakes workflows. This improves both predictive accuracy and interpretability, essential for clinical decision-making. Using open-access real-world datasets and fine-tuned open-source LLM backbones ensures rapid adoption and extension by the global research community, accelerating precision oncology and improving patient outcomes. Our models outperform strong baselines (e.g., Med42, Meditron, OpenBio) across binary classification, survival regression, and reasoning quality, with GRPO-CoT achieving the best F1, lowest error, and most coherent rationales. We also find that interpretability metrics correlate strongly with accuracy, supporting that structured reasoning promotes generalization. These findings mark a shift from black-box prediction to reasoning-aware clinical AI, vital in oncology, where transparency is critical. Future directions include expanding to other clinical tasks (e.g., treatment recommendation, disease progression), incorporating multi-modal data like imaging and genomics, and exploring human-in-the-loop RL setups for validation and refinement. Our work lays the foundation for systems that not only **know** medicine, but can **reason** with it.

References

2000. *Front Matter*, i–xii. John Wiley & Sons, Ltd. ISBN 9780471722144.

Alsentzer, E.; Murphy, J.; Boag, W.; Weng, W.-H.; Jindi, D.; Naumann, T.; and McDermott, M. 2019. Publicly Available Clinical BERT Embeddings. In Rumshisky, A.; Roberts, K.; Bethard, S.; and Naumann, T., eds., *Proceedings of the 2nd Clinical Natural Language Processing Workshop*, 72–78. Minneapolis, Minnesota, USA: Association for Computational Linguistics.

Ankit Pal, M. S. 2024. OpenBioLLMs: Advancing Open-Source Large Language Models for Healthcare and Life Sciences. <https://huggingface.co/aaditya/OpenBioLLM-Llama3-70B>.

Arasteh, H.; and Lotfinia, M. 2023. Large Language Models Streamline Automated Machine Learning for Clinical Studies. *arXiv*.

Boag, W.; Sergeeva, E.; Kulshreshtha, S.; Szolovits, P.; Rumshisky, A.; and Naumann, T. 2018. CliNER 2.0: Accessible and Accurate Clinical Concept Extraction.

Breiman, L. 2001. Random Forests. *Machine Learning*, 45(1): 5–32.

Caruana, R.; Lou, Y.; Gehrke, J.; Koch, P.; Sturm, M.; and Elhadad, N. 2015. Intelligible Models for HealthCare: Predicting Pneumonia Risk and Hospital 30-day Readmission. In *Proceedings of the 21th ACM SIGKDD International Conference on Knowledge Discovery and Data Mining*, KDD '15, 1721–1730. New York, NY, USA: Association for Computing Machinery. ISBN 9781450336642.

Chen, B.; and Brown, M. 2023. Language Models are Few-Shot Learners for Prognostic Prediction. *arXiv*.

Chen, M.; Liu, Y.; Liu, L.; Zhang, X.; and Lee, Y.-K. 2020. Predicting treatment success in various diseases through genetic and clinical data integration. *Nature Medicine*, 26(3): 302–312.

Chen, Z.; Hernández-Cano, A.; Romanou, A.; Bonnet, A.; Matoba, K.; Salvi, F.; Pagliardini, M.; Fan, S.; Köpf, A.; Mohtashami, A.; Sallinen, A.; Sakhaeirad, A.; Swamy, V.; Krawczuk, I.; Bayazit, D.; Marmet, A.; Montariol, S.; Hartley, M.-A.; Jaggi, M.; and Bosselut, A. 2023. MEDITRON-70B: Scaling Medical Pretraining for Large Language Models. *arXiv:2311.16079*.

Christophe, C.; Kanithi, P. K.; Raha, T.; Khan, S.; and Pimentel, M. A. 2024. Med42-v2: A Suite of Clinical LLMs. *arXiv:arXiv:2408.06142*.

Clusmann, J.; Kolbinger, F. R.; Muti, H. S.; Carrero, Z. I.; Eckardt, J.-N.; Laleh, N. G.; Löffler, C. M. L.; Schwarzkopf, S.-C.; Unger, M.; Veldhuizen, G. P.; Wagner, S. J.; and Kather, J. N. 2023. The future landscape of large language models in medicine. *Communications Medicine*, 3(1): 141.

Cox, D. R. 1992. *Regression Models and Life-Tables*, 527–541. New York, NY: Springer New York. ISBN 978-1-4612-4380-9.

Dao, T. 2024. FlashAttention-2: Faster Attention with Better Parallelism and Work Partitioning. In *The Twelfth International Conference on Learning Representations*.

DeepSeek-AI; and et. al., D. G. 2025. DeepSeek-R1: Incentivizing Reasoning Capability in LLMs via Reinforcement Learning. *arXiv:2501.12948*.

Esteva, A.; Robicquet, A.; Ramsundar, B.; Kuleshov, V.; De-Pristo, M.; Chou, K.; Cui, C.; Corrado, G.; Thrun, S.; and Dean, J. 2019. A guide to deep learning in healthcare. *Nat. Med.*, 25(1): 24–29.

et. al., A. G. 2024. The Llama 3 Herd of Models. *arXiv:2407.21783*.

Fong, C. J.; Pichotta, K.; Tran, T. N.; Waters, M.; Fu, T.; Pirun, M.; Altoe, M. L.; Mastrogiacomo, B.; Luthra, A.; Ahmed, M. S.; Pasha, A.; Kohli, A.; Lim, R.; Pollard, T.; Moore, D.; Gross, B. E.; Wang, A.; Chennault, C.; Kundra, R.; Madupuri, R.; de Brujin, I.; Lisman, A.; Chatila, W. K.; Nandakumar, S.; Begum, A.; Rose, D.; Kehl, K. L.; Schrag, D.; Berger, M. F.; Carrot-Zhang, J.; Razavi, P.; Li, B. T.; Stetson, P. D.; Schultz, N.; and Jee, J. 2024a. Abstract 3892: Systematic generation of a clinicogenomic harmonized oncologic real-world dataset (MSK-CHORD). *Cancer Research*.

Fong, C. J.; Pichotta, K.; Waters, M.; Fu, T.; Pirun, M.; Altoe, M. L.; Mastrogiacomo, B.; Luthra, A.; Ahmed, M. S.; Pasha, A.; Kohli, A.; Lim, R.; Pollard, T.; Moore, D.; Gross, B.; Wang, A.; Chennault, C.; Kundra, R.; Madupuri, R.; de Brujin, I.; Lisman, A.; Chatila, W. K.; Nandakumar, S.; Begum, A.; Rose, D.; Kehl, K. L.; Schrag, D.; Berger, M. F.; Carrot-Zhang, J.; Razavi, P.; Li, B. T.; Stetson, P. D.; Schultz, N.; and Jee, J. 2024b. Abstract 3892: Systematic generation of a clinicogenomic harmonized oncologic real-world dataset (MSK-CHORD). *Cancer Research*.

Friedman, J. H. 2001. Greedy function approximation: A gradient boosting machine. *The Annals of Statistics*, 29(5): 1189 – 1232.

Gema, A. P.; Minervini, P.; Daines, L.; Hope, T.; and Alex, B. 2024. Parameter-Efficient Fine-Tuning of LLaMA for the Clinical Domain. *arXiv:2307.03042*.

Gu, C., Desai. 2024a. Health System-Scale Language Models Are All-Purpose Prediction Engines. *Nature*, 600(7884): 43–58.

Gu, C., Desai. 2024b. Probabilistic Medical Predictions of Large Language Models. *npj Digital Medicine*, 7(3): 65–78.

Hanahan, D.; and Weinberg, R. A. 2011. Hallmarks of cancer: the next generation. *Cell*, 144(5): 646–674.

He, Y.; Tang, B.; and Wang, X. 2024. Generative Models for Automatic Medical Decision Rule Extraction from Text. In Al-Onaizan, Y.; Bansal, M.; and Chen, Y.-N., eds., *Proceedings of the 2024 Conference on Empirical Methods in Natural Language Processing*, 7034–7048. Miami, Florida, USA: Association for Computational Linguistics.

Henriksson, A.; Pawar, Y.; Hedberg, P.; and Nauclér, P. 2023. Multimodal fine-tuning of clinical language models for predicting COVID-19 outcomes. *Artificial Intelligence in Medicine*, 146: 102695.

Hou, Y.; Bert, C.; Gomaa, A.; Lahmer, G.; Hoefler, D.; Weissmann, T.; Voigt, R.; Schubert, P.; Schmitter, C.; Depardon, A.; Semrau, S.; Maier, A.; Fietkau, R.;

Huang, Y.; and Putz, F. 2024. Fine-Tuning a Local LLaMA-3 Large Language Model for Automated Privacy-Preserving Physician Letter Generation in Radiation Oncology. *arXiv*:2408.10715.

Hu, L.; Liu, L.; Yang, S.; Chen, X.; Xiao, H.; Li, M.; Zhou, P.; Ali, M. A.; and Wang, D. 2024. A Hopfieldian View-based Interpretation for Chain-of-Thought Reasoning. *arXiv*:2406.12255.

Huang, J.; Gu, S.; Hou, L.; Wu, Y.; Wang, X.; Yu, H.; and Han, J. 2023. Large Language Models Can Self-Improve. In Bouamor, H.; Pino, J.; and Bali, K., eds., *Proceedings of the 2023 Conference on Empirical Methods in Natural Language Processing*, 1051–1068. Singapore: Association for Computational Linguistics.

Jee, J.; and et. al, C. J. F. 2024. Automated real-world data integration improves cancer outcome prediction. *Visual education*.

Jee, J.; Fong, C.; Pichotta, K.; Tran, T. N.; Luthra, A.; Waters, M.; Fu, C.; Altoe, M.; Liu, S.-Y.; Maron, S. B.; Ahmed, M.; Kim, S.; Pirun, M.; Chatila, W. K.; de Brujin, I.; and Pasha, A. 2024. Automated real-world data integration improves cancer outcome prediction. *Nature*, 636(8043): 728–736.

Jensen, P. B.; Jensen, L. J.; and Brunak, S. 2012. Mining electronic health records: towards better research applications and clinical care. *Nat. Rev. Genet.*, 13(6): 395–405.

Jiang, Z.; Zhang, Y.; Wang, X.; Liu, R.; and Zhou, Z. 2022. A machine learning-based approach to predict the success of cancer immunotherapy. *Journal of Immunotherapy*, 45(3): 105–116.

Kazachkov, I. V. 2015. The Theory and Applications of Parametric Excitation and Suppression of Oscillations in Continua: State of the Art. *arXiv*:1510.06986.

Kim, J.; Lee, S.-H.; Jung, Y.; and Jeon, Y.-J. 2023. Predictive modeling of treatment outcomes for chronic diseases using electronic health records. *Journal of Medical Systems*, 47(1): 15.

Kraljevic, Z.; Yeung, J. A.; Bean, D.; Teo, J.; and Dobson, R. J. 2024. Large Language Models for Medical Forecasting – Foresight 2. *arXiv*:2412.10848.

Langbein, S. H.; Krzyzinski, M.; Spytek, M.; Baniecki, H.; Biecek, P.; and Wright, M. N. 2024. Interpretable Machine Learning for Survival Analysis. *arXiv.org*, abs/2403.10250.

Li, J.; Cao, P.; Wang, C.; Jin, Z.; Chen, Y.; Zeng, D.; Liu, K.; and Zhao, J. 2024. Focus on Your Question! Interpreting and Mitigating Toxic CoT Problems in Commonsense Reasoning. *arXiv*:2402.18344.

Lin, C.-Y. 2004. ROUGE: A Package for Automatic Evaluation of Summaries. In *Text Summarization Branches Out*, 74–81. Barcelona, Spain: Association for Computational Linguistics.

Litjens, G.; Kooi, T.; Bejnordi, B. E.; Setio, A. A. A.; Ciompi, F.; Ghafoorian, M.; van der Laak, J. A.; van Ginneken, B.; and Sánchez, C. I. 2017. A survey on deep learning in medical image analysis. *Medical Image Analysis*, 42: 60–88.

Liu, P.; Bai, Y.; Wang, Z.; Lin, X.; Zhou, X.; Liu, S.; et al. 2023. Policy Optimization by Population-based Reinforcement Learning for Language Agents. *arXiv preprint arXiv*:2309.13683.

Loshchilov, I.; and Hutter, F. 2019. Decoupled Weight Decay Regularization. In *International Conference on Learning Representations*.

Lu, H.; Liu, W.; Zhang, B.; Wang, B.; Dong, K.; Liu, B.; Sun, J.; Ren, T.; Li, Z.; Yang, H.; Sun, Y.; Deng, C.; Xu, H.; Xie, Z.; and Ruan, C. 2024. DeepSeek-VL: Towards Real-World Vision-Language Understanding. *arXiv*:2403.05525.

Lu, P.; Mishra, S.; Xia, T.; Qiu, L.; Chang, K.-W.; Zhu, S.-C.; Tafjord, O.; Clark, P.; and Kalyan, A. 2022. Learn to Explain: Multimodal Reasoning via Thought Chains for Science Question Answering. *arXiv*:2209.09513.

Lyu, D.; Wang, X.; Chen, Y.; and Wang, F. 2024. Language model and its interpretability in biomedicine: A scoping review. *iScience*, 27(4): 109334.

MacQueen, J. 1967. Some methods for classification and analysis of multivariate observations. In *Proceedings of the fifth Berkeley symposium on mathematical statistics and probability*, volume 1, 281–297. Oakland, CA, USA.

Marusyk, A.; Almendro, V.; and Polyak, K. 2012. Intra-tumour heterogeneity: a looking glass for cancer? *Nat. Rev. Cancer*, 12(5): 323–334.

Mondillo, G.; Colosimo, S.; Perrotta, A.; Frattolillo, V.; and Masino, M. 2025. Comparative Evaluation of Advanced AI Reasoning Models in Pediatric Clinical Decision Support: ChatGPT O1 vs. DeepSeek-R1. *medRxiv*.

Naik, P.; Feldman, W.; and Hope, E. 2021. Literature-Augmented Clinical Outcome Prediction. *arXiv*.

Nazi, Z. A.; and Peng, W. 2024. Large Language Models in Healthcare and Medical Domain: A Review. *Informatics*, 11(3).

Ong, J.; Chang, S. Y.-H.; Wasswa, W.; Butte, A.; Shah, N.; Chew, L.; Liu, N.; Doshi-Velez, F.; Lu, W.; Savulescu, J.; and Ting, D. 2024. Medical Ethics of Large Language Models in Medicine. *NEJM AI*, 1.

OpenAI; and et. al., J. A. 2024. GPT-4 Technical Report. *arXiv*:2303.08774.

Papineni, K.; Roukos, S.; Ward, T.; and Zhu, W.-J. 2002. BLEU: a method for automatic evaluation of machine translation. In *Proceedings of the 40th annual meeting on association for computational linguistics*, 311–318. Association for Computational Linguistics.

Phan, D.; Hoffman, M. D.; Dohan, D.; Douglas, S.; Le, T. A.; Parisi, A.; Sountsov, P.; Sutton, C.; Vikram, S.; and Saurous, R. A. 2023. Training Chain-of-Thought via Latent-Variable Inference. *arXiv*:2312.02179.

PMC, S. . 2023. Leveraging Large Language Models for Decision Support in Precision Oncology. *Journal of Precision Medicine*, 1(2): 123–135.

Radford, A.; Wu, J.; Child, R.; Luan, D.; Amodei, D.; and Sutskever, I. 2019. Language Models are Unsupervised Multitask Learners.

Rajkomar, A.; Oren, E.; Chen, K.; Dai, A. M.; Hajaj, N.; Hardt, M.; Liu, P. J.; Liu, X.; Marcus, J.; Sun, M.; Sundberg, P.; Yee, H.; Zhang, K.; Zhang, Y.; Flores, G.; Duggan, G. E.; Irvine, J.; Le, Q.; Litsch, K.; Mossin, A.; Tansuwan, J.; Wang, D.; Wexler, J.; Wilson, J.; Ludwig, D.; Volchenboum, S. L.; Chou, K.; Pearson, M.; Madabushi, S.; Shah, N. H.; Butte, A. J.; Howell, M. D.; Cui, C.; Corrado, G. S.; and Dean, J. 2018. Scalable and accurate deep learning with electronic health records. *NPJ Digit. Med.*, 1(1): 18.

Reimers, N.; and Gurevych, I. 2019. Sentence-BERT: Sentence Embeddings using Siamese BERT-Networks. In *Proceedings of the 2019 Conference on Empirical Methods in Natural Language Processing*. Association for Computational Linguistics.

Schulman, J.; Wolski, F.; Dhariwal, P.; Radford, A.; and Klimov, O. 2017. Proximal Policy Optimization Algorithms. *arXiv:1707.06347*.

Shao, Z.; Wang, P.; Zhu, Q.; Xu, R.; Song, J.; Bi, X.; Zhang, H.; Zhang, M.; Li, Y. K.; Wu, Y.; and Guo, D. 2024. DeepSeekMath: Pushing the Limits of Mathematical Reasoning in Open Language Models. *arXiv e-prints*, arXiv:2402.03300.

Shao, Z.; Wang, P.; Zhu, Q.; Xu, R.; Song, J.; Bi, X.; Zhang, H.; Zhang, M.; Li, Y. K.; Wu, Y.; and Guo, D. 2024. DeepSeekMath: Pushing the Limits of Mathematical Reasoning in Open Language Models. *arXiv:2402.03300*.

Shoham, R. 2023. CPLLM: Clinical Prediction with Large Language Models. *arXiv*.

Singh, A.; and Brown, M. 2024. Mitigating Bias in Medical AI: Strategies for Fair Large Language Models. *Artificial Intelligence in Medicine*, 78(3): 231–245.

Sonntag, D.; and Profitlich, H.-J. 2019. An architecture of open-source tools to combine textual information extraction, faceted search and information visualisation. *Artificial Intelligence in Medicine*, 93: 13–28. Extracting and Processing of Rich Semantics from Medical Texts.

Tian, H.; and Patel, S. 2023. Explainable AI for Large Language Models in Healthcare. *Journal of Biomedical Informatics*, 142(1): 102937.

Tonekaboni, S.; Joshi, S.; McCradden, M. D.; and Goldenberg, A. 2019. What Clinicians Want: Contextualizing Explainable Machine Learning for Clinical End Use. In Doshi-Velez, F.; Fackler, J.; Jung, K.; Kale, D.; Ranganath, R.; Wallace, B.; and Wiens, J., eds., *Proceedings of the 4th Machine Learning for Healthcare Conference*, volume 106 of *Proceedings of Machine Learning Research*, 359–380. PMLR.

Topol, E. J. 2019. High-performance medicine: the convergence of human and artificial intelligence. *Nat. Med.*, 25(1): 44–56.

Torkamani, A.; Ochoa, J.; Matthews, P. M.; Boustany, N.; and Olsson, M. 2020. Predicting treatment success in personalized medicine: Current challenges and future perspectives. *Journal of Personalized Medicine*, 10(1): 4.

Wang, L.; and Zhao, Q. 2024. Transformer-Based Personalized Treatment Recommendation in Precision Medicine. *Nature Medicine*, 30(5): 456–472.

Wei, J.; Wang, X.; Schuurmans, D.; Bosma, M.; Ichter, B.; Xia, F.; Chi, E. H.; Le, Q. V.; and Zhou, D. 2022. Chain-of-thought prompting elicits reasoning in large language models. In *Proceedings of the 36th International Conference on Neural Information Processing Systems*, NIPS '22. Red Hook, NY, USA: Curran Associates Inc. ISBN 9781713871088.

Xue, A.; and Abraham, J. 2024. Predicting Postoperative Risks Using Large Language Models. *arXiv*.

Yala, A.; Mikhael, P. G.; Strand, F.; Lin, G.; Smith, K.; Wan, Y.-L.; Lamb, L.; Hughes, K.; Lehman, C.; and Barzilay, R. 2021. Toward robust mammography-based models for breast cancer risk. *Sci. Transl. Med.*, 13(578): eaba4373.

Yang, Y.; Yu, J.; Fu, Z.; Zhang, K.; Yu, T.; Wang, X.; Jiang, H.; Lv, J.; Huang, Q.; and Han, W. 2024. Token-Mixer: Bind Image and Text in One Embedding Space for Medical Image Reporting. *IEEE Transactions on Medical Imaging*, 43(11): 4017–4028.

Yao, S.; Zhao, J.; Yu, D.; Narasimhan, K.; Cao, Y.; and Li, Y. 2022. ReAct: Synergizing Reasoning and Acting in Language Models. *arXiv preprint arXiv:2210.03629*.

Zakka, S.; and Chaurasia, A. 2023. Almanac: Retrieval-Augmented Language Models for Clinical Medicine. *arXiv*.

Zhang, C.; Chen, Y.; Huang, J.-K.; Wu, X.; Li, L.-J.; Yao, W.; Tersoff, J.; and Shih, C.-K. 2016. Visualizing band offsets and edge states in bilayer–monolayer transition metal dichalcogenides lateral heterojunction. *Nature Communications*, 7(1): 10349.

Zhang, T.; Kishore, V.; Wu, F.; Weinberger, K. Q.; and Artzi, Y. 2020. BERTScore: Evaluating Text Generation with BERT. *arXiv:1904.09675*.

Zheng, P.; Xu, L.; and Fu, Y. 2024. Multimodal Clinical Trial Outcome Prediction with Large Language Models. *arXiv*.

Zhou, J.; Han, Z.; Shi, J.; Wang, N.; Li, H.; and Yang, L. 2021. Predicting the therapeutic efficacy of immunotherapy using multi-modal data: A deep learning approach. *Nature Communications*, 12(1): 6957.

Zhu, Y.; Wang, Z.; Gao, J.; Tong, Y.; An, J.; Liao, W.; Harrison, E. M.; Ma, L.; and Pan, C. 2024. Prompting Large Language Models for Zero-Shot Clinical Prediction with Structured Longitudinal Electronic Health Record Data. *arXiv:2402.01713*.

Zitu, M. M.; Le, T. D.; Duong, T.; Haddadan, S.; Garcia, M.; Amorrtu, R.; Zhao, Y.; Rollison, D. E.; and Thieu, T. 2024. Large language models in cancer: potentials, risks, and safeguards. *BJR—Artificial Intelligence*, 2(1): ubae019.

1. Input and Model Outputs

Here, we present an input prompt example and the corresponding responses generated by different models, including reasoning, prognosis comment, and final survival prediction.

Input Prompt

```
1 ### Instruction:  
2 You are a cancer clinical outcome  
3 prediction model. Based on the  
4 patient data provided, predict the  
5 treatment outcome. Focus on key  
6 clinical factors such as disease  
7 stage, tumor site(s), patient age,  
8 smoking history, cancer type, and  
9 treatment details.  
10  
11 Your response should include:  
12 1. Step-by-step reasoning using relevant  
13 clinical knowledge.  
14 2. A concise comment on the patient's  
15 prognosis.  
16 3. Final prediction in the specified  
17 format.  
18  
19 Format your response as follows:  
20 <reasoning>  
21 [Step-by-step explanation]  
22 </reasoning>  
23  
24 <comment>  
25 [Prognosis summary]  
26 </comment>  
27  
28 <prediction>  
29 Overall Survival Status: '0:LIVING' or  
30 '1:DECEASED'  
31 Estimated Overall Survival (months): [  
32 float value]  
33 </prediction>  
34  
35 ### Input:  
36 Clinical Attributes: Cancer Stage 1-3;  
37 Current Age=60; Sex=Female; Smoking  
38 History=Former/Current Smoker  
39 Tumor Sites: Adrenal Glands, Bone, CNS/  
40 Brain, Intra Abdominal, Lung, Lymph  
41 Node  
42 Treatments:  
43 - Chemotherapy: CARBOPLATIN, CISPLATIN,  
44 ETOPOSIDE, GEMCITABINE, PEMETREXED,  
45 Days: 20-819  
46 - Immunotherapy: NIVOLUMAB, Days:  
47 363-440  
48 - Radiation Therapy: Days -1135  
49 Sample-Specific Information (Non-Small  
50 Cell Lung Cancer):  
51 - Clinical Group: 3A  
52 - Cancer Type Detailed: Lung  
53 Adenocarcinoma  
54 - Sample Type: Primary  
55 - MSI Type: Stable  
56 - MSI Score: 0.08
```

Our LLaMa3 (GRPO) Output

```
1 <reasoning>  
2 Step 1: Assess patient demographics and  
3 risk factors. Age 60 and smoking  
4 history (former/current smoker) are  
5 associated with poorer outcomes in  
6 NSCLC due to comorbidities and  
7 potential tumor aggressiveness.  
8 Step 2: Evaluate tumor burden and  
9 metastatic spread. Multiple distant  
10 sites (adrenal glands, bone, CNS/  
11 brain, lymph nodes) suggest advanced  
12 disease, even though the clinical  
13 stage is listed as 1-3. This  
14 discrepancy raises uncertainty about  
15 whether the staging reflects initial  
16 diagnosis or progression.  
17 Step 3: Analyze chemotherapy regimens.  
18 Initial cisplatin/etoposide (likely  
19 first-line for small cell lung cancer)  
20 followed by carboplatin/pemetrexed  
21 (standard for non-squamous NSCLC)  
22 suggests possible disease progression  
23 or recurrence requiring regimen  
24 changes. Later gemcitabine and  
25 abbreviated carboplatin/pemetrexed  
26 cycles may indicate poor tolerance or  
27 rapid progression.  
28 Step 4: Consider immunotherapy timing.  
29 Nivolumab was administered after  
30 chemotherapy, potentially as second-  
31 line therapy. However, its  
32 discontinuation at day 440 (short  
33 duration) raises questions about  
34 efficacy or toxicity, which could  
35 negatively impact survival.  
36 Step 5: Note absence of radiation/  
37 investigational therapies. Lack of  
38 localized radiation for CNS/brain  
39 metastases or investigational agents  
40 may reflect limited options or poor  
41 performance status, both poor  
42 prognostic indicators.  
43 Step 6: Synthesize factors. High  
44 metastatic burden, multi-line  
45 chemotherapy resistance,  
46 immunotherapy discontinuation, and  
47 smoking-related comorbidities  
48 collectively suggest aggressive  
49 disease biology and limited  
50 therapeutic response.  
51 </reasoning>  
52  
53 <comment>  
54 Uncertainties include: 1) Potential  
55 staging inconsistency (Stage 1-3 vs.  
56 multi-organ metastases), 2) Exact  
57 reasons for chemotherapy regimen  
58 changes (toxicity vs. progression),  
59 3) Performance status during  
60 treatments, and 4) Biomarker status (e.g., PD-L1, EGFR) not provided.  
61 These gaps limit precision in outcome  
62 attribution.
```

```

12 </comment>
13
14 <prediction>
15 Overall Survival Status: 1:DECEASED
16 Estimated Overall Survival (months):
17 27.9
18 </prediction>

```

Our Med42 Base (GRPO) Output

```

1 <reasoning>
2 Step 1: Assessed patient age (60) and
   smoking history (former/current
   smoker), both of which are negative
   prognostic factors in NSCLC due to
   increased comorbidity risks and
   potential for aggressive tumor
   biology.
3 Step 2: Evaluated tumor sites (adrenal
   glands, bone, CNS/brain, etc.).
   Widespread metastases suggest
   advanced disease progression, which
   typically correlates with poorer
   outcomes. However, the listed stage
   (1-3) conflicts with the presence of
   distant metastases, creating
   uncertainty about staging accuracy.
4 Step 3: Analyzed chemotherapy regimens.
   Early use of cisplatin/etoposide (
   first-line for NSCLC) followed by
   carboplatin/pemetrexed (second-line)
   and later gemcitabine/carboplatin/
   pemetrexed suggests disease
   progression through multiple lines of
   therapy, indicating treatment
   resistance.
5 Step 4: Noted immunotherapy (nivolumab)
   administered late in the timeline (
   days 363-440). While nivolumab can
   improve survival in NSCLC, its
   delayed initiation and short duration
   (78 days) may reflect limited
   efficacy or intolerance, reducing its
   prognostic benefit.
6 Step 5: Observed absence of radiation/
   investigational therapies,
   potentially limiting disease control
   options. Lack of radiation for CNS/
   brain metastases (if present) could
   worsen neurological complications.
7 Step 6: Considered clinical group 3A (
   locally advanced) conflicting with
   metastatic sites. If metastases
   developed post-initial staging, this
   would imply rapid progression and
   poor response to systemic therapy.
8 Step 7: Synthesized factors: Advanced
   age, smoking history, multi-organ
   metastases, and sequential
   chemotherapy failures collectively
   suggest aggressive disease biology
   with limited therapeutic options,
   leading to poor prognosis.
9 </reasoning>
10

```

```

11 <comment>
12 Uncertainties include staging
   inconsistency (metastases vs. stage
   1-3), exact timing of metastasis
   development, and reasons for
   immunotherapy discontinuation. The
   absence of biomarker data (e.g., PD-
   L1 status) limits assessment of
   nivolumab's potential impact.
   Conflicting staging data complicates
   interpretation of disease trajectory.
13 </comment>
14
15 <prediction>
16 Overall Survival Status: 1:DECEASED
17 Estimated Overall Survival (months):
18 33.0
19 </prediction>

```

Baseline Med42 Output

```

1
2 <reasoning>
3 1. The patient has advanced Non-Small
   Cell Lung Cancer (NSCLC) with
   multiple metastatic sites (Adrenal
   Glands, Bone, CNS/Brain, Intra
   Abdominal, Lung, Lymph Node),
   indicating an aggressive disease
   course.
4 2. The patient's age (60) is within the
   average range for NSCLC patients, but
   the presence of multiple metastases
   and a high clinical group (3A)
   suggest a poorer prognosis.
5 3. The patient is a former/current
   smoker, which increases the risk of
   treatment-related complications and
   reduces overall survival.
6 4. The treatment regimen includes
   multiple lines of chemotherapy (
   CISPLATIN, ETOPOSIDE, CARBOPLATIN,
   PEMETREXED, GEMCITABINE) and
   immunotherapy (NIVOLUMAB), indicating
   a comprehensive and aggressive
   treatment approach.
7 5. The absence of radiation therapy may
   limit local control, but the
   inclusion of immunotherapy may
   enhance systemic control.
8 </reasoning>
9
10 <comment>
11 The patient's prognosis is guarded due
   to the advanced stage of NSCLC,
   multiple metastatic sites, and
   smoking history.
12 </comment>
13
14 <prediction>
15 Overall Survival Status: 1:DECEASED
16 Estimated Overall Survival (months):
17 12.4
18 </prediction>

```

2. Dataset Description

We utilize the **MSK-CHORD dataset** (Jee and et. al 2024; Fong et al. 2024b), a comprehensive clinical oncology dataset curated by Memorial Sloan Kettering Cancer Center (MSKCC). The dataset is publicly accessible via the cBio-Portal and includes structured clinical records of patients diagnosed with various cancer types, including lung cancer. The dataset provides a rich repository of **patient demographics, disease progression, treatment history, molecular profiling, and survival outcomes**, making it highly suitable for predictive modeling in clinical oncology.

Dataset Scope and Sampling

The MSK-CHORD dataset consists of **24,950 patient records**, encompassing detailed clinical, genomic, and treatment information. To enhance model reasoning and interpretability, we generate **chain of thought (CoT) explanations for 80% samples**, which serve as a cold-start training set for alignment in outcome prediction tasks.

Data Structure and Key Features

Each patient record is stored in **JSON format**, encapsulating structured information on the following categories:

- **Demographics:** Age, sex, race, ethnicity, and smoking history.
- **Clinical Data:** Cancer type, tumor site, disease stage (highest recorded), and molecular markers such as PD-L1 expression, HER2, and HR status.
- **Diagnosis History:** Initial and follow-up diagnoses, including cancer progression probabilities derived from radiology reports and pathology findings.
- **Treatment Modalities:**
 - **Chemotherapy:** Agents administered, including CYCLOPHOSPHAMIDE, FLUOROURACIL, METHOTREXATE, CISPLATIN, ETOPOSIDE, and CARBOPLATIN.
 - **Immunotherapy:** Use of checkpoint inhibitors such as NIVOLUMAB.
 - **Investigational Therapies:** Records of participation in experimental treatment trials.
 - **Radiation Therapy:** Details on radiation sessions, including initiation time relative to diagnosis.
 - **Surgery:** Procedures performed and sample extractions.
- **Laboratory Tests:** Biomarkers such as CEA and CA 15-3 levels tracked over time.
- **Genomic Data:** Tumor mutation burden (TMB), microsatellite stability (MSI), and fraction of genome altered.
- **Survival Outcomes:** Overall survival status (0: LIVING or 1: DECEASED) and estimated survival duration in months.

Data Processing for LLM-Based Outcome Prediction

To predict cancer treatment outcomes, we transform the structured JSON data into a **natural language prompt** suitable for **large language models (LLMs)**. Each prompt consists of:

- A **task description** instructing the model to predict survival status and duration.
- A cancer-type-specific **patient clinical summary**, created using dynamically selected attributes.

The model is tasked with predicting:

1. **Overall survival status** (0 : LIVING or 1 : DECEASED)
2. **Estimated survival duration in months** (continuous value)

Chain-of-Thought Prompt Construction and Generation

To enable clinically grounded survival prediction, we developed a reasoning-aligned Chain-of-Thought generation framework that integrates structured patient information with cancer-type-specific attribute selection.

Cancer-Specific Attribute Selection

To reduce token overhead and improve clinical relevance, we restrict the attributes included in each patient summary based on the diagnosed cancer type. Attribute inclusion is guided by priority scores derived from attribute metadata and cancer-specific biological relevance.

Example 1: Breast Cancer. We retain hormone receptor status attributes such as HER2, ER, PR, and HR, as well as key tumor markers like CA15-3. Stage, age, and metastasis site are also included. Sample-specific attributes like Cancer Type Detailed and Clinical Summary are selected if informative.

Example 2: Non-Small Cell Lung Cancer (NSCLC). We prioritize smoking history, biomarker mutations (e.g., EGFR, ALK), and expression levels like PD-L1. We also include general attributes such as stage and age, along with sex and key lab values like CEA.

Cancer-to-attribute mappings are constructed using keyword matching and attribute scope filters (Patient vs Sample) derived from structured metadata. This ensures that each summary focuses on clinically meaningful features while minimizing irrelevant information.

Patient Summary Construction

To generate clinically interpretable reasoning traces, we first construct structured patient summaries from raw MSK-CHORD records. These summaries are designed to be concise, cancer-type-specific, and optimized for reasoning relevance. The system extracts and formats patient information into logical sections, prioritizing high-utility attributes while filtering irrelevant ones based on metadata flags and disease-specific heuristics.

- **Clinical Attributes:** Includes general prognostic factors such as stage, age, sex, and smoking history, along with other high-priority features from the patient metadata.

- **Biomarkers:** Selects molecular markers relevant to the diagnosed cancer type, such as HER2, PD-L1, or PSA.
- **Tumor Sites:** Extracts metastasis indicators from affirmative tumor site flags.
- **Treatments:** Summarizes therapies (e.g., chemotherapy, immunotherapy, radiation) including the time intervals during which they were administered.
- **Sample-Specific Information:** Extracts histological, anatomical, and diagnostic attributes specific to cancer samples.
- **Key Tumor Markers:** Analyzes lab test trends (e.g., CEA, CA19-9) using linear regression to describe progression over time.

These elements are composed into a natural-language summary, which is passed to a language model alongside survival outcome data. This allows the model to reason clinically over structured features, producing interpretable justifications for its predictions.

Reasoning Model Training and Chain-of-Thought Generation

We leverage **large-scale models such as DeepSeek R1** (Mondillo et al. 2025; DeepSeek-AI and et. al. 2025) to generate **chain-of-thought (CoT) reasoning traces** (Lu et al. 2022; Hu et al. 2024; Li et al. 2024) for interpretability and model alignment. CoT explanations are generated for **all samples**, ensuring robust supervision while maintaining computational efficiency. The reasoning process involves:

1. **Assessing cancer stage and diagnosis**, to determine baseline prognosis and identify likely disease trajectory.
2. **Evaluating patient-specific factors**, such as age, sex, and implied treatment eligibility.
3. **Reviewing biomarker patterns and tumor marker trends**, assessing disease progression or treatment response through temporal lab data.
4. **Analyzing treatment regimens and timing**, including systemic and local therapies (chemotherapy, immunotherapy, radiation, and investigational agents) to evaluate therapeutic intensity and intent.
5. **Weighing clinical evidence holistically**, synthesizing inputs across all dimensions to estimate likely survival outcome.

Additionally, each prediction is accompanied by a **commentary on clinical uncertainties**, highlighting gaps such as missing data, ambiguous staging, or incomplete treatment details (Fong et al. 2024a). This enhances interpretability and clinical relevance. The **MSK-CHORD dataset** serves as a robust foundation for **treatment outcome prediction in oncology** (Fong et al. 2024a). Our approach—combining structured clinical data, LLM-driven reasoning, and interpretability mechanisms—paves the way for improved decision support in personalized cancer treatment.

Chain-of-Thought Evaluation via Embedding-Based Metrics

To assess the quality of Chain-of-Thought (CoT) explanations generated across 25,000 patient records, we conducted an automatic evaluation using sentence-transformer-based semantic similarity. Each CoT trace was assessed for: (i) step-to-summary relevance, (ii) intra-step coherence, and (iii) prompt repetition, using cosine similarity scores computed from BERT-based sentence embeddings.

Table 6: Evaluation of Chain-of-Thought (CoT) reasoning traces across 25,000 cancer patient summaries using BERT-based similarity metrics.

Metric	Mean	Std Dev	Min	Max
AVERAGE RELEVANCE	0.537	0.048	0.332	0.745
MINIMUM RELEVANCE	0.394	0.081	0.008	0.721
AVERAGE COHERENCE	0.463	0.067	0.179	0.812
MAX PROMPT OVERLAP	0.306	0.041	0.160	0.460
NUMBER OF STEPS	6.10	0.92	3.00	14.00

These results reveal three key findings. First, the **average relevance score of 0.537** indicates that the CoT traces are generally well-grounded in the patient data, supporting the fidelity of model reasoning. Second, the **average coherence of 0.463** suggests that consecutive reasoning steps maintain logical continuity, though further improvements are possible. Third, a **low prompt overlap score of 0.306** demonstrates that the model rarely reuses instruction phrasing, instead generating novel, context-specific explanations.

To further understand variation across clinical contexts, we stratified the CoT evaluation metrics by cancer type. Table 7 reports the mean and standard deviation of each score across the five major cancer types in our dataset.

3. Method

Generalized Reward Policy Optimization (GRPO)

Generalized Reward Policy Optimization (GRPO) (Shao et al. 2024) is a reinforcement learning framework that optimizes policy models by directly incorporating reward signals into the policy update process without requiring a separate critic network. Instead of estimating a value function for each action, GRPO leverages a group-based approach where, for each input, a group of outputs is sampled from a reference (or old) policy. The rewards of these outputs are compared relative to each other, providing a robust baseline that reduces variance during training.

At the core of GRPO is the objective function:

$$J_{GRPO}(\theta) = \mathbb{E} \left[\frac{1}{G} \sum_{i=1}^G \left(\min \left(\frac{\pi_\theta(o_i|q)}{\pi_{\theta_{old}}(o_i|q)} A_i, \right. \right. \right. \\ \left. \left. \left. \text{clip} \left(\frac{\pi_\theta(o_i|q)}{\pi_{\theta_{old}}(o_i|q)}, 1 - \epsilon, 1 + \epsilon \right) A_i \right) \right. \right. \\ \left. \left. \left. - \beta D_{KL}(\pi_\theta \| \pi_{ref}) \right) \right], \quad (2)$$

Table 7: Mean BERT-based evaluation metrics for Chain-of-Thought (CoT) quality across different cancer types.

Cancer Type	Avg Relevance	Min Relevance	Avg Coherence	Prompt Overlap	Steps
BREAST CANCER	0.525	0.393	0.447	0.308	6.22
COLORECTAL CANCER	0.525	0.378	0.458	0.305	6.33
NSCLC (LUNG)	0.538	0.410	0.465	0.295	5.88
PANCREATIC CANCER	0.567	0.397	0.465	0.301	6.26
PROSTATE CANCER	0.547	0.382	0.491	0.333	5.92

where: The expectation is with respect to $q \sim P(Q)$, $\{o_i\}_{i=1}^G \sim \pi_{\theta_{old}}(O|q)$

- π_θ is the current policy,
- $\pi_{\theta_{old}}$ is the policy used to sample the outputs,
- A_i is the advantage for the i -th output,
- ϵ and β are hyperparameters,
- $D_{KL}(\pi_\theta \parallel \pi_{ref})$ is a regularization term that penalizes deviation from a reference policy π_{ref} .

The KL divergence term is defined as:

$$D_{KL}(\pi_\theta \parallel \pi_{ref}) = \frac{\pi_{ref}(o_i|q)}{\pi_\theta(o_i|q)} - \log \frac{\pi_{ref}(o_i|q)}{\pi_\theta(o_i|q)} - 1. \quad (3)$$

The advantage A_i is computed as:

$$A_i = \frac{r_i - \text{mean}(\{r_1, r_2, \dots, r_G\})}{\text{std}(\{r_1, r_2, \dots, r_G\})}, \quad (4)$$

where r_i is the reward associated with the i -th output, and the mean and standard deviation are computed over the group of sampled outputs.

This formulation enables efficient and stable policy updates by using group-level relative rewards to guide learning, thereby eliminating the need for a separate critic model while ensuring data efficiency and robust convergence.

4. Experiment

Hardware and Optimization Details

All experiments were conducted using 4× NVIDIA A100 GPUs (40GB, PCIe) with PyTorch 2.1 and Hugging Face Transformers (v4.39). Training used bfloat16 precision with FlashAttention 2 enabled (Dao 2024). Input sequences were truncated or packed to a maximum length of 1024 tokens. Gradient checkpointing was used to reduce memory usage, enabling a batch size of 4 samples per GPU. With 4-way data parallelism and 4 gradient accumulation steps, the effective global batch size was 16. A fixed random seed (42) was used for all runs to ensure reproducibility.

SFT Training Configuration

The following configuration was used for all SFT experiments:

- **Optimizer:** AdamW with ($\beta_1 = 0.9, \beta_2 = 0.999$)
- **Learning Rate Schedule:** Cosine annealing with:
 - Initial learning rate = 1×10^{-4}
 - Minimum learning rate = 1×10^{-5}

- Warmup ratio = 0.05
- **Weight Decay:** 0.1
- **Batch Size:** 16 (accumulated to 64 with gradient accumulation)
- **Precision:** Mixed-precision (FP16)
- **Epochs:** 2 total
- **Checkpointing:** Saved every 100 steps
- **Evaluation Frequency:** Every 100 steps
- **Loss:** Multi-task objective (binary classification + regression) computed over the autoregressive token output

GRPO Training Configuration

The following hyperparameters were used for GRPO-based reinforcement tuning:

- **Optimizer:** AdamW (Loshchilov and Hutter 2019)
- **Learning Rate:** 5×10^{-5} with cosine decay
- **Warmup Steps:** 5
- **Weight Decay:** 0.1
- **GRPO-specific Parameters:**
 - PPO Clip $\epsilon = 0.1$
 - Discount Factor $\gamma = 0.99$
 - GAE (Generalized Advantage Estimation) $\lambda = 0.95$ (Schulman et al. 2017)
 - Value Loss Coefficient: 0.5
 - Entropy Bonus: 0.01
- **Training:** 3 epochs
- **Batch Size:** Gradient accumulation over 4 steps (effective batch size = 16)
- **Checkpointing:** Every 200 steps
- **Evaluation Frequency:** Every 200 steps
- **Datasets:** Cold-start subset (5K) and full MSK-CHORD (Jee et al. 2024)

All GRPO runs used the same reasoning-aware reward design described in Section , with training stabilizing after 2–3 epochs.

We observed consistent convergence within 2 epochs across both LLaMa3 and Med42 models, without signs of overfitting.

The results demonstrate meaningful variation in reasoning quality across cancer types. Pancreatic cancer CoTs achieved the highest average relevance (0.567), suggesting strong grounding in the patient summary, while prostate

cancer exhibited the most coherent step transitions (0.491). Lung cancer CoTs had slightly fewer steps on average (5.88), whereas colorectal cancer traces were the most verbose (6.33). Notably, all cancer types maintained low prompt overlap (≈ 0.34), reinforcing that the model’s reasoning remains distinct from the original instructions. These findings indicate that our CoT generation strategy adapts well across cancer types while preserving clinical fidelity and coherence.

These gains are further validated by ROC curves (Figure 7), where CoT-guided models show stronger class separability and sharper rises in true positive rates. Notably, OURS (LLAMA3)-COT and OURS (MED42)-COT outperform all MED42 variants. Overall, these results underscore two key insights: (1) CoT prompting enhances both predictive accuracy and interpretability in survival prediction, and (2) GRPO-based alignment offers a promising route for tailoring biomedical LLMs to clinical decision-making.

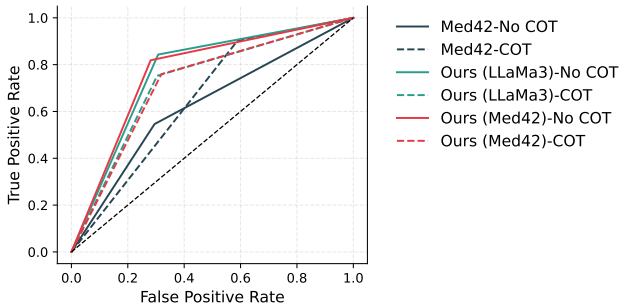


Figure 7: ROC Curves for survival status prediction across CoT and non-CoT models. Our GRPO-aligned LLaMa3 variant achieves the most robust separation.

Table 8: ROUGE score breakdown for all models under Chain-of-Thought (CoT) prompting.

Model	ROUGE-1	ROUGE-2	ROUGE-L
MEDITRON	0.115	0.025	0.082
OPENBIO	0.311	0.091	0.172
MED42	0.447	0.150	0.241
DEEPEEK R1	0.381	0.101	0.166
OURS (MED42) -GRPO	0.645 0.652	0.304 0.308	0.363 0.368
OURS (LLAMA3) -GRPO	0.644 0.653	0.304 0.310	0.364 0.370

In terms of robustness, our models demonstrated zero failure cases across all evaluated settings. Specifically, both our Med42- and LLaMa3-based models achieved **100% response rates** under Chain-of-Thought (CoT) prompting, including after GRPO fine-tuning. In contrast, baseline models such as MEDITRON and OPENBIO exhibited substantial gaps, failing to produce predictions for 1911 and 1854 samples respectively when CoT was enabled. Even without

CoT prompting, MEDITRON missed 28 predictions, while MED42 had only 6 failures. Our GRPO-optimized variants further reinforced reliability, yielding zero missing predictions in all configurations. These findings underscore the enhanced stability and completeness of our framework, particularly under structured reasoning scenarios.

Table 9: Count of missing predictions per model, separated by Chain-of-Thought (CoT) prompting.

Model	Without CoT	With CoT
MEDITRON	28	1911
OPENBIO	0	1854
MED42	6	82
OURS (MED42)	0	0
<i>Ours (Med42)(GRPO)</i>	–	0
OURS (LLAMA3)	0	0
<i>Ours (LLaMa3)(GRPO)</i>	–	0

5. Code and CoT Dataset

The code used for our experiments is available at: <https://github.com/OncoReason/Clinical-Reasoning-LLMs>

The Chain-of-Thought dataset we curated is available on Hugging Face: <https://huggingface.co/datasets/oncollm/cancer-reasoning-traces>